Kinetics of N_2O_5 Hydrolysis on Secondary Organic Aerosol and Mixed Ammonium Bisulfate−Secondary Organic Aerosol Particles

Egda N. Escorcia,*,† Steven J. Sjostedt,‡ and Jonathan P. D. Abbatt†

Department of Chemistry, University of Toronto, Toronto, and Science and Technology Branch, Environment Canada, North York, Ontario, Canada

Received: August 15, 2010; Revised Manuscript Received: October 20, 2010

The kinetics of the hydrolysis reaction of N_2O_5 on secondary organic aerosol (SOA) produced through the ozonolysis of α-pinene and on mixed ammonium bisulfate−SOA particles was investigated using an entrained aerosol flow tube coupled to a chemical ionization mass spectrometer. We report room temperature uptake coefficients, γ, on ammonium bisulfate and SOA particles at 50% relative humidity of $1.5 \times 10^{-2} \pm 1.5 \times 10^{-3}$ and $1.5 \times 10^{-4} \pm 2 \times 10^{-5}$, respectively. For the mixed ammonium bisulfate−SOA particles, γ decreased from $2.6 \times 10^{-3} \pm 4 \times 10^{-4}$ to $3.0 \times 10^{-4} \pm 3 \times 10^{-5}$ as the SOA mass fraction increased from 9 to 79, indicating a strong suppression in γ with the addition of organic material. There is an order-of-magnitude reduction in the uptake coefficient with the smallest amount of SOA material present and smaller additional reductions with increasing aerosol organic content. This newly coated organic layer may either decrease the mass accommodation coefficient of N_2O_5 onto the particle or hinder the dissolution and diffusion of N_2O_5 into the remainder of the aerosol after it has been accommodated onto the surface. The former corresponds to a surface effect and the latter to bulk processes. The low value of the uptake coefficient on pure SOA particles will likely make N_2O_5 hydrolysis insignificant on such an aerosol, but atmospheric chemistry models need to account for the role that organics may play in suppressing the kinetics of this reaction on mixed organic−inorganic particles.

1. Introduction

Nitric oxide and nitrogen dioxide, NO and NO_2, respectively, are primary reactants in the production of tropospheric O_3, a harmful greenhouse gas and oxidant. Collectively referred to as NO_x, these species are recycled when O_3 is produced during the day, but may ultimately be lost at night if they enter a different pathway to form N_2O_5, a nocturnal NO_x reservoir. N_2O_5 can subsequently react with water on aerosol surfaces to yield HNO_3:

$$N_2O_{5(g)} + H_2O_{aerosols} \rightarrow 2HNO_3 \qquad \text{(R1)}$$

Given that NO_x, and consequently O_3, concentrations are affected by the overall production, depletion, and chemistry of N_2O_5, this heterogeneous reaction (R1) has been extensively studied under a variety of conditions to determine its varying influence on NO_x and O_3 budgets.[1−5] For example, Evans and Jacob demonstrated that upon the inclusion of N_2O_5 heterogeneous loss in the global chemical transport model, GEOS-CHEM, NO_x and O_3 concentrations decreased by 53.5% and 9.4%, respectively, on a global average.[1] By incorporating five distinct aerosol substrates (dust, sulfate, organic carbon, black carbon, and sea salt) and their diverse effects on N_2O_5 hydrolysis into their model, the resulting O_3 and NO_x distributions showed better agreement with previously reported data than with estimates from models that had not included heterogeneous aerosol chemistry in their calculations.[1] This study confirmed the general predictions of Dentener and Crutzen[2] performed more than a decade earlier.

The uptake coefficient, γ, is the probability that a reaction will occur between a N_2O_5 gas molecule and an aerosol surface when these two species collide. Mozurkewich and Calvert demonstrated in 1988 that N_2O_5 uptake on aqueous ammonium bisulfate (NH_4HSO_4) and sulfuric acid (H_2SO_4) particles was faster than through a homogeneous reaction under similar atmospheric conditions.[6] As such, to follow were a number of studies which examined various organic and inorganic aqueous systems at varying relative humidities (RHs), including, for example, work performed on aqueous ammonium sulfate,[7,8] sodium bisulfate and sodium nitrate,[9,10] malonic acid and other organic acids,[11,12] and NaCl/artificial seawater[13−15] aerosol. The reported uptake coefficients for the hydrolysis of N_2O_5 on these substrates vary from 0.0005 to 0.05 and are dependent on several factors, including aerosol size, phase, and especially relative humidity. The trend observed for most aqueous systems shows an increase in γ with increasing relative humidity,[6−14] with suppressions in γ occurring most notably as a result of organic substrates or coatings,[8,13,16−19] and high concentrations of nitrate present in the aerosol bulk.[9,10]

Both of these effects have been investigated by several researchers in an attempt to parametrize and express each in a concise manner.[9,10,20] Mentel et al. have described the ionic mechanism of N_2O_5 hydrolysis and related it to a "nitrate effect", essentially demonstrating that aerosols containing large amounts of NO_3^-, as well as small concentrations of water, can lead to a suppression in γ; e.g., an increase in $[NO_3^-]$ from 13.4 to 158 mol/kg decreased γ from 0.018 to 0.0002.[9,10] A recent study by Bertram and Thornton outlines a systematic parametrization of the influences of H_2O, nitrate, and chloride concentrations on the uptake coefficient of N_2O_5 for internally mixed particles

* To whom correspondence should be addressed. Phone: (416) 946-7359. E-mail: egda.escorcia@utoronto.ca.
† University of Toronto.
‡ Environment Canada.

10.1021/jp107721v
Published on Web 12/02/2010

containing these species.[20] They assume the formation of a protonated nitric acid intermediate ($H_2ONO_2^+$), which can then react with H_2O, nitrate, or chloride present in the aerosols to either promote or suppress N_2O_5 reactivity. Bertram and Thornton concluded that either a water limitation exists in the reaction of $H_2ONO_2^+$ with water or nitrate or mass accommodation of N_2O_5 is water dependent.[20] In addition, they illustrated that increasing nitrate concentrations in the particles led to a decrease in the uptake coefficients measured and that low water and high nitrate concentrations worked in synergy to produce lower γ values. The researchers derived an expression for γ that is dependent on H_2O, nitrate, and chloride concentrations, where the importance of each is regulated by the rate coefficients of the reaction of $H_2ONO_2^+$ with each species.[20]

The mechanism by which submonolayer-thick organic films on particles decrease the uptake coefficient has yet to be parametrized, but it is likely that they inhibit the mass accommodation of N_2O_5 within the outer layers of the aerosol particle.[16−19] Thornton and Abbatt were the first to address the effects of organic monolayers by coating artificial seawater with hexanoic acid.[13] The results indicated that the organic coating suppressed γ by a factor of 3 from 0.024 to 0.008, but it was undetermined whether the surfactant monolayers had the greatest impact on the mass accommodation coefficient or the rate of reaction at the interface.[13] Other studies illustrate an equivalent pattern, with the greatest suppressions in γ occurring for ordered films composed of large organic molecules and high organic coating concentrations.[18,19] For example, Cosman et al.[19,21] demonstrated that a straight chain surfactant (1-octadecanol) decreased the uptake coefficient of N_2O_5 onto 60 wt % aqueous sulfuric acid to a significant degree, while a branched monolayer (phytanic acid) affected γ only slightly. Branched monolayers do not pack efficiently on an aerosol surface and thus do not decrease the uptake coefficient as much as straight chain monolayers because the spaces present between branched monolayers allow N_2O_5 to diffuse more quickly.[18,19,21]

In general, organic monolayers have been shown to both enhance and suppress uptake of gases to liquid. In particular, researchers have monitored the entry of different gases, such as HCl and HBr, onto sulfuric acid particles through 1-butanol and hexanol films.[22] In these cases, the chemistry does not follow that of N_2O_5 uptake in that the organic films actually enhance rather than impede acidic uptake. It is believed that the hydroxyl groups on the organic layer help facilitate this uptake.[22] On the other hand, organic films are also known to suppress the uptake of ammonia,[23] water,[24] nitric acid,[25] and acetic acid.[26]

Another class of N_2O_5 studies have considered the role of organics on the kinetics when present in large quantities in an organic particle, much greater than a monolayer. In particular, field work conducted by Bertram and Thornton at Boulder, CO, and Seattle, WA, has indicated that a large organic presence in/on aerosols decreases γ to a significant degree: the results indicate that increasing organic-to-sulfate ratios affect γ by decreasing the ability of the aerosols to take up water and by enhancing the strength of the nitrate effect.[27] Brown et al. have also indicated through ambient measurements obtained as part of the New England Air Quality Study (NEAQS) that organics may suppress reactivity.[28−30]

From a laboratory perspective, two studies have examined the effects of adding substantial quantities of organics to inorganic substrates, i.e., the work of Folkers et al.[8] and Badger et al.[31] In particular, Folkers, Mentel, and Wahner investigated the reaction of N_2O_5 with ammonium bisulfate aerosols coated with secondary organic aerosol (SOA) material produced through the ozonolysis of α-pinene.[8] The researchers reported a decrease in γ from 0.0187 to 0.0034 at 60% RH when an SOA coating, approximately 15 nm thick, was added to the particles.[8] Likewise, Badger et al. report decreases in γ by a factor of 9, 3.8, and 2.3 at 25%, 50%, and 70% RH, respectively, with the addition of only 6% humic acid by mass to ammonium sulfate solutions, from which particles were formed by atomization.[31] These substantial suppressions were interpreted as being due to an effect on the mass accommodation coefficient of N_2O_5 on these organic-containing particles.

The motivations for the research presented in this paper were twofold. First was the need to supplement and expand the limited literature data available on the heterogeneous reaction of N_2O_5 with particles containing organics. Second was the desire to better understand the mechanism of suppression, which occurs upon the addition of an organic layer to aerosol, and how variable amounts of this new organic material affect N_2O_5 uptake. In particular, two mechanisms—a surface-dependent process and a bulk-dependent process—are possible. Given the knowledge that tropospheric particles are commonly composed of a mixture of inorganic and secondary organic material,[32] we investigated the reaction of N_2O_5 with ammonium bisulfate aerosols mixed with SOA produced through the reaction of O_3 and α-pinene at 45−50% RH. α-Pinene was chosen since it is the most common monoterpene, a class of compounds that efficiently leads to SOA formation. Although SOA formed from oxidation of monoterpenes in the laboratory is not as oxidized as that found in the field, it remains the best model substance we have for ambient SOA.

To contrast the behavior observed with these two-component aerosols, we also present the uptake coefficients obtained for single-component ammonium bisulfate at 50% RH and SOA at 0%, 30%, and 50% RH. These experiments extend the work performed by Folkers et al.[8] but using a different experimental technique, an aerosol flow tube coupled to a newly built chemical ionization mass spectrometer (CIMS). We also employ the new CIMS N_2O_5 detection method of $I^- \cdot N_2O_5$ cluster formation, as first demonstrated by Kercher et al., rather than the more common approach of NO_3^- detection.[33]

2. Experimental Methods

Figure 1 illustrates the overall experimental setup for the two-component aerosol experiments. The layouts for each of the single-component experiments were similar to that shown in Figure 1, except that the SOA and ammonium bisulfate single-component trials did not require the atomizer and O_3 denuder, respectively. In addition, the single-component experiments only required one mixing flow tube. We note that the overall experimental approach is similar to that which we have used in a previous study.[11] Details pertaining to the novel aspects of this study are provided below.

2.1. Chemical Ionization Mass Spectrometer. The chemical ionization mass spectrometer (Figure 2) is a home-built instrument constructed according to the designs of G. Huey and D. Tanner from the Georgia Institute of Technology. The instrument, along with all essential electronics and accessory items, is mounted on a wheeled 104 cm × 61 cm × 114 cm aluminum boxed frame. It is divided into four differentially pumped chambers, the ion molecule region (IMR), the collisional dissociation chamber (CDC), the intermediate chamber (IC), and the multiplier chamber (MC). This instrument contains four critical orifices, one each leading into the subsequent chamber, two octupole ion guides (THS Instruments, LLC), one quadrupole (Extrel Core Mass Spectrometers, 9.5 mm diameter rods),

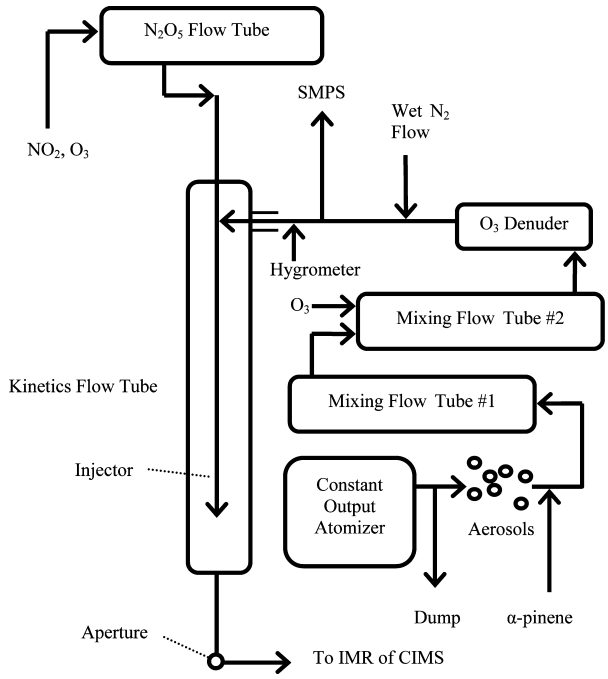

Figure 1. Schematic depicting the overall experimental setup for the two-component aerosol experiments for N_2O_5 hydrolysis. Both the ammonium bisulfate and SOA single-component experiments required only one mixing flow tube and additional flows to regulate the RH.

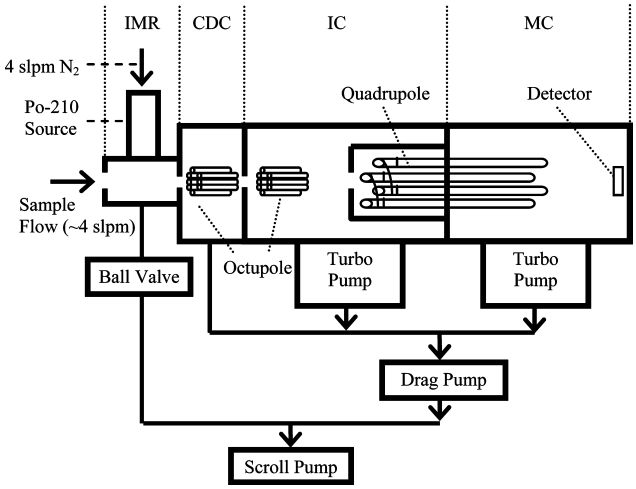

Figure 2. Schematic of the CIMS displaying the four differentially pumped chambers: ion molecule region (IMR), collisional dissociation chamber (CDC), intermediate chamber (IC), and multiplier chamber (MC).

and an on-axis electron multiplier detector (ITT Power Solutions, Inc., 7550 M channel electron multiplier). The pressures, when in operational mode, are 45, 0.1, 1×10^{-4}, and 1×10^{-6} Torr in the IMR, CDC, IC, and MC, respectively. Ions entering the CIMS follow a trajectory from the inlet into the IMR, CDC, IC, and last MC, where they are detected. The CIMS samples a total of 7−8 standard liters per minute (slpm) through the IMR, with 4 slpm N_2 pertaining to the flow required to transport the reagent ion and the other half corresponding to sample flow. The sample flow for these experiments was not as large as 4 slpm, so a N_2O_5-free makeup flow was added. The reagent ion flow enters the IMR through a side cavity positioned after the first critical orifice, whereas the sample flow enters the IMR via an inlet fixed with Teflon tubing and then proceeds to the first aperture.

2.2. Aerosol Generation. Ammonium bisulfate aerosols for the single-component and two-component experiments were produced from 20 and 2 wt % solutions, respectively, of ammonium bisulfate (Sigma-Aldrich, 307602) using a constant output atomizer (TSI 3076). A dump line was added from the exit of the atomizer to vent excess particles for all ammonium bisulfate experiments and to maintain the system at atmospheric pressure. For the NH_4HSO_4 single-component experiments only, the aerosol passed through a silica gel dryer before entering a mixing flow tube where both a wet (i.e., through a water bubbler) and a dry flow of N_2 were added to regulate the RH in the system. These wet and dry flows were regulated by mass flow controllers (MFCs), and varied from 600 to 800 and from 300 to 400 standard cubic centimeters per minute (sccm), respectively, to achieve the desired relative humidity. The resulting flow moved directly to the kinetics flow tube and entered through a side inlet at the top.

The two-component experiments did not require a dryer, as the flow from the atomizer, in addition to a single wet flow of N_2 (∼750 sccm, regulated by a needle valve and rotometer) added before the kinetics flow tube, was employed to fix the RH to a value of 50% (Figure 1). Two preparatory flow tubes were required for these experiments: the first for the mixing of ammonium bisulfate aerosol and α-pinene gas and the second for the mixing of the contents of the first flow tube with O_3. The flow exiting the second flow tube passed through an O_3 denuder before entering the kinetics flow tube. α-Pinene gas was produced by passing a small (up to 30 sccm) dry N_2 flow through a fritted glass bubbler containing α-pinene liquid (Fluka, 99%) held at room temperature. A N_2 dilution flow was also added after the bubbler (500−700 sccm) to produce a range of α-pinene concentrations. Ozone was produced by passing a flow of O_2 (up to 30 sccm) over a 22.9 cm long (mercury) Hg Pen-Ray lamp (UVP, LLC) to photolyze O_2 to O_3 at a wavelength of 185 nm. Considering experimental procedures and gas flows similar to those outlined by George and Abbatt,[34] we estimate that O_3 and α-pinene mixing ratios for these experiments were up to 20 and 50 ppm, respectively.

The particles produced for the SOA single-component experiments employed only one flow tube for the mixing of α-pinene and O_3. SOA exiting this flow tube also passed through an O_3 denuder before entering the kinetics flow tube. In this case, the dump line to the atmosphere was positioned at the top of the kinetics flow tube to vent excess aerosol. All flows for these experiments were regulated by MFCs, and the concentrations were slightly higher (by no more than a factor of 2) than those of the mixed experiments. Additional wet and dry N_2 flows were added to the main flow just before the kinetics flow tube to regulate the RH. These flows were added in various ratios (total flow of 2 slpm) to produce conditions of 0%, 30%, and 50% RH.

It should be noted that with the exception of minor changes to gas flows the experimental conditions leading to the production of the SOA were held constant throughout the study in an attempt to also keep the composition of the SOA constant. As such, the change in reactivity is a result of the changing mass fraction of the SOA component and/or RH, rather than a result of changing SOA composition. Also, we assume that all the SOA is formed by gas-phase reactions followed by gas-to-particle conversion. Given the low solubility of monoterpenes, we do not anticipate that much organic oxidation is occurring in the condensed phase.

All aerosol surface areas were characterized by means of a scanning mobility particle sizer (SMPS) system consisting of a

differential mobility analyzer (DMA; TSI 3080-3081) and condensation particle counter (CPC; TSI 3025A). The SMPS system sampled from a tee located immediately before the top of the kinetics flow tube.

2.3. N_2O_5 Generation and Detection. N_2O_5 was produced in situ in a 50 cm long glass flow tube through the dark reaction of O_3 and NO_2. O_3 was produced through the photolysis of O_2 (up to 4 sccm) flowing over a small Hg Pen-Ray lamp. NO_2 was supplied from a NO_2 cylinder custom-ordered from Linde BOC Gases consisting of 2000 ppm NO_2 in N_2. NO_2 was added in excess (~13−27 ppm in the kinetics flow tube) to ensure that the equilibrium shifted toward the product (N_2O_5) rather than toward the reactants (NO_3 and NO_2). The $[N_2O_5]/[NO_3]$ ratio was approximated as being roughly 10^4, thus indicating that N_2O_5 concentrations were much larger than NO_3 concentrations. Once formed, N_2O_5 then proceeded to the kinetics flow tube, entered via a 6 mm o.d. (~4.5 mm i.d.) injector at the top, and exited along with the main flow at the bottom toward the IMR of the CIMS.

We use I^- as the CIMS reagent ion, produced from methyl iodide, CH_3I (Sigma Aldrich, 99%), following exposure to a polonium-210 radioactive source.[33] It is delivered from a home-built permeation tube (6.4 cm long) that is composed of Teflon tubing (PFA, 3 mm i.d., 5 mm o.d.) plugged at the ends with a 1 cm long Teflon rod (PTFE, 0.32 cm diameter) and crimped shut with stainless steel tubing (0.56 cm o.d., 0.52 cm i.d.). The permeation tube is placed within an aluminum block and heated to 70 °C by a temperature controller (Omega Engineering Inc., CN1A series). As the permeation tube is heated, CH_3I diffuses through the Teflon walls and is carried by a 4 slpm N_2 flow toward the ^{210}Po source and then to the IMR of the CIMS.

N_2O_5 was detected by monitoring the reagent ion cluster, $I^-\cdot N_2O_5$, rather than NO_3^-, as shown in the reactions below:[33]

$$I^- + N_2O_5 \rightarrow NO_3^- + INO_2 \quad \text{(R2)}$$

$$I^- + H_2O + M \rightarrow I^-\cdot H_2O + M \quad \text{(R3)}$$

$$I^- + N_2O_5 + M \rightarrow I^-\cdot N_2O_5 + M \quad \text{(R4)}$$

$$I^-\cdot H_2O + N_2O_5 \rightarrow I^-\cdot N_2O_5 + H_2O \quad \text{(R5)}$$

Dissociative charge transfer (reaction R2) is problematic, as I^- can also react with HNO_3 to yield an equivalent NO_3^- ion, thus requiring the subtraction of a chemical background from all measurements. Ion cluster formation (reaction R4 and R5),[33] however, is accompanied by minimal background.

Calibrations were performed as outlined by Thornton et al.,[11] by producing N_2O_5 through the reaction of excess NO_2 and O_3 and then trapping it in an ethanol/liquid N_2 slush bath (163 K). The trap was then warmed and the N_2O_5 signal was monitored while a small, known flow passed through the trap and into a larger dilution flow. The resulting sensitivity and detection limit of this instrument for the $I^-\cdot N_2O_5$ cluster are 0.024 Hz/pptv and 100 pptv (S/N = 2), respectively, for an I^- signal level of 125 kHz. The lowest reagent ion signals used in the work were 15 kHz.

2.4. Kinetics Measurements and Analysis Approach. The kinetics flow tube, mounted vertically, is 90 cm long with an inner radius of 3.0 cm. Wall losses of N_2O_5 were minimized by maintaining the flow tube at atmospheric pressure and coating the interior walls with halocarbon wax. It was also covered with aluminum foil to eliminate the possibility of N_2O_5 photolysis and fitted with a glass injector, 6 mm o.d. (~4.5 mm i.d.) and 120 cm long. The relative humidity was monitored at the top entrance to the kinetics flow tube with a hygrometer (VWR).

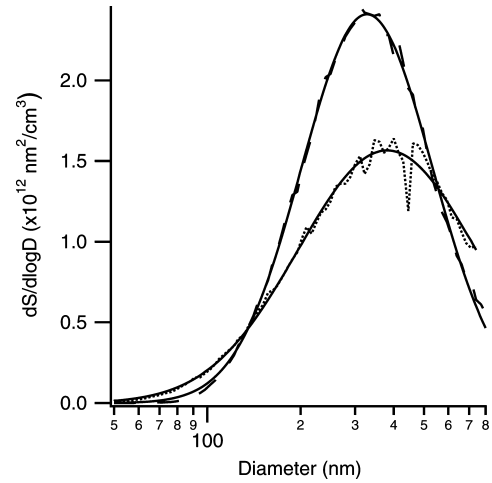

Figure 3. Surface area size distributions of ammonium bisulfate particles and SOA combined (dotted line) and ammonium bisulfate particles without the addition of SOA (dashed line). Given that approximately 20% of the total surface area for the two-component experiments was not measured by the SMPS system, the distributions were corrected using log-normal fits (solid lines).

Kinetics measurements were performed by varying the position of the injector inside the flow tube. It was pulled out systematically in 15 cm increments every 3 min while the ion signal and aerosol surface area were monitored. These surface areas were determined by averaging seven distributions recorded sequentially during the time of the kinetics measurements. Given that several distributions for the two-component and ammonium bisulfate single-component experiments were not fully measured by the SMPS, the missing portions were assessed using log-normal fits (see Figure 3). The ammonium bisulfate to SOA mass fractions were determined from the SMPS volume measurements, in particular by measuring the volume of the ammonium bisulfate aerosol with and without SOA present. Although the hygroscopic growth factor at 50% RH for the ozonolysis of α-pinene[35] is essentially 1.0, it is ~1.22 ± 0.02 for ammonium bisulfate[36−38] under these conditions. As such, the volumes measured for the ammonium bisulfate particles were reduced by a factor of 1.22 (see ref 36−38) to account for the presence of water. These corrected volumes were then used to convert to mass fractions assuming a density of 1.78 and 1.41 g/cm^3 for ammonium bisulfate[39] and SOA[40] produced through the ozonolysis of α-pinene, respectively.

This approach of determining the inorganic mass fraction assumes that each component in the aerosol has an associated amount of water, a quantity which is not altered by the mixing of the components; i.e., they independently take up water.[41,42] Also known as the Zdanovskii−Stokes−Robinson (ZSR) assumption, it describes the final hygroscopic growth factor of the mixed component aerosol as a linear combination of the hygroscopic growth factors and volume fractions of the individual components.[41,42] The ZSR method has been experimentally validated by, for example, Badger et al.,[43] Brooks et al.,[44] and Gysel et al.[45] These researchers investigated the hygroscopic growths of mixed humic acid−ammonium sulfate[43,44] particles and aged air masses[45] using tandem differential mobility analysis (TDMA) to demonstrate the validity of this technique.

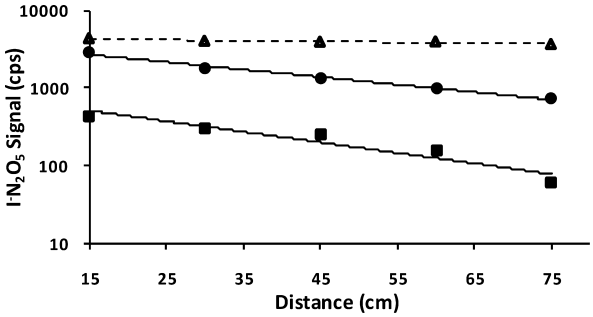

Figure 4. Corrected (i.e., background-subtracted) decay plots of the $I^- \cdot N_2O_5$ signal (cps) vs injector position (cm) at 50% RH in the absence (triangles, dashed line) and presence (solid lines) of aerosols. The decays correspond to an aerosol surface area of 1.2×10^{-4} and 1.5×10^{-2} cm^2/cm^3 for ammonium bisulfate (squares) and SOA (circles) produced through the ozonolysis of α-pinene, respectively.

Background control runs were required to determine wall losses of N_2O_5 and thus were conducted in the absence of aerosols, but at relative humidity conditions equivalent to those during experimental runs. These background runs were usually performed at the beginning and end of a set of kinetic runs. Since N_2O_5 was monitored via ion cluster formation ($I^- \cdot N_2O_5$), the background signal subtracted at this mass-to-charge ratio corresponded to the signal of a small chemical background and multiplier noise present during sampling times. That is, despite having nitric acid present in the flow tube as a product of the reaction, it gave rise to no background at *m*/*z* 235. The background values we observed via this detection method ranged from 7 to 25 cps or from 1.2 to 4.2 ppb N_2O_5, respectively, for any kinetic run. Using essentially the same experimental setup as Thornton et al.,[11] the losses of aerosol in the flow tube are estimated to be less than 10%. Also, as in that previous study,[11] measurements were not taken within 15 cm of the end of the flow tube to ensure an adequate mixing length of N_2O_5 into the flow, as well as to establish laminar flow. The N_2O_5 mixing ratios normally present during experiments varied from 20 to 150, from 350 to 750, and from 70 to 330 ppb for the ammonium bisulfate (AB), SOA, and AB−SOA experiments, respectively.

Figure 4 displays N_2O_5 decays both in the absence (triangles, dashed line) and in the presence (solid lines) of aerosol at 45−50% RH. First-order kinetics were observed in all experiments. The ammonium bisulfate and SOA single-component decays shown correspond to a surface area (of each respective aerosol type) of 1.2×10^{-4} and 1.5×10^{-2} cm^2/cm^3, respectively. As can be seen, the decay of ammonium bisulfate (squares) is similar to that of SOA (circles), but for two very distinct surface areas.

The flow in the kinetics flow tube was held constant during each experimental run by a critical orifice in a Teflon disk situated within an UltraTorr fitting placed at the bottom of the flow tube. Depending on the pinhole used, the total flow varied from 1000 to 1600 sccm. The slopes of the decays shown in Figure 4 are converted into pseudo-first-order rate constants (k^I) using the bulk flow velocity in the flow tube, which varied from 0.64 to 1.02 cm s^{-1}. k^I values are then corrected to account for nonplug flow conditions using the method as described by Brown.[46] The second-order rate constant (k^{II}) corresponds to the slope of a graph of k^I vs aerosol surface area, thus leading to the determination of γ using the following expression:

$$k^{II} = \frac{\gamma_{N_2O_5}\omega_{N_2O_5}SA}{4} \quad \text{(E1)}$$

where $\omega_{N_2O_5}$ is the mean molecular speed of N_2O_5 and SA is the total aerosol surface area. For the magnitude of the uptake coefficients measured in this work, the gas-phase diffusion limitation, as assessed using the Fuchs−Sutugin[47] corrections, is no more than 3%.

3. Results

The surface area distributions for the SOA single-component experiments were log-normal distributions that peaked around 400 nm and produced very large surface areas. The ammonium bisulfate single-component distributions were wider, peaked at a smaller diameter, roughly 300 nm, and corresponded to smaller overall surface areas. Figure 3 shows distributions obtained for two-component system experiments, both for ammonium bisulfate particles with SOA added (dotted line) and for the ammonium bisulfate particles without SOA present (dashed line); i.e., the SOA was removed by turning off ozone and α-pinene in the SOA-generation system while the carrier flows (N_2) remained unchanged. The log-normal fits are shown as solid lines. As can be seen, the ammonium bisulfate distribution peaks at 325 nm, whereas the distribution for the ammonium bisulfate to SOA (41:59 AB−SOA by mass) two-component particle peaks at 375 nm. Upon the addition of SOA to the ammonium bisulfate particles, the aerosol distributions became wider and shifted slightly to larger sizes. We estimate that errors in the total aerosol surface area measurements as determined by the SMPS system are on the order of ±25%, which includes possible errors from the CPC, possible losses within the kinetics flow tube, and the errors associated with estimating (through log-normal fits) the amount of surface area that we did not directly measure.

Figure 5 displays the first-order rate constants for N_2O_5 on the particles versus the total aerosol surface area for the AB and SOA single-component decays, where the rate constants have been corrected for wall loss and laminar flow effects by the approach of Brown.[46] Similar plots of the mixed aerosol experiments are not included in this graph, but were determined using the same procedure as with the single-component systems. The uptake coefficients for the two-component runs, however, were determined from a two-point relationship, one measurement corresponding to the wall-loss background rate constant with zero aerosol surface area and the second to the rate constant associated with the two-component aerosol surface area. We used this approach because it was not practical to maintain a constant ratio of AB to SOA within the particle over a wide range of total aerosol surface areas. Nevertheless, the kinetics obtained on the single-component species (Figure 5) verify that our overall kinetics approach was valid, with a highly linear relation between the magnitude of the first-order decay constant and aerosol surface area. Therefore, we feel confident that this relationship also holds in the runs with the mixed AB−SOA particles.

A total of six different AB−SOA mixed aerosol compositions were studied, in addition to AB (50% RH) and SOA single-component (0%, 30%, and 50% RH) particles, as indicated in Table 1. γ values and the RH conditions for each respective aerosol type are also summarized in Table 1, along with the uncertainties in the resulting uptake coefficients. The uncertainties quoted for the single-component kinetics arise from an unweighted least-squares fit to the data in Figure 5. For the

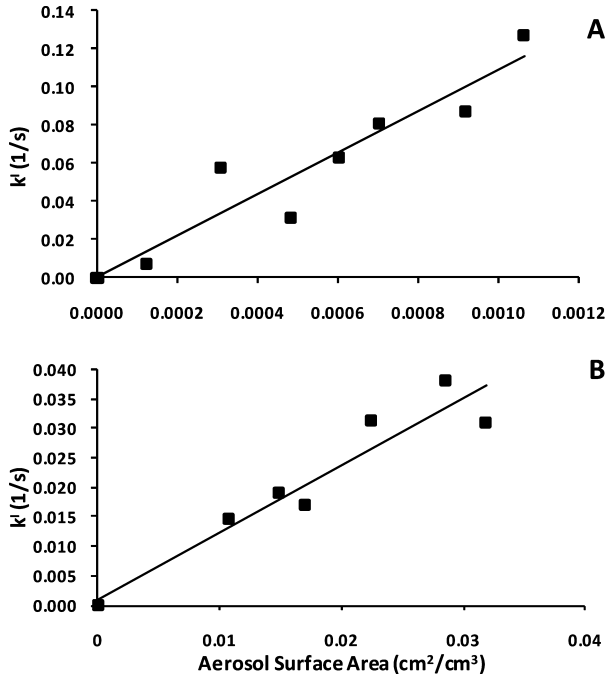

Figure 5. Pseudo-first-order rate constant vs aerosol surface area for the hydrolysis of N_2O_5 on ammonium bisulfate (A) and SOA (B) particles at 50% RH. Ammonium bisulfate aerosols were generated from a 20 wt % solution using an atomizer, and the SOA particles were produced through the ozonolysis of α-pinene. The rate constants have been corrected for wall loss using the Brown approach.[46]

TABLE 1: Uptake Coefficients, γ, for N_2O_5 Hydrolysis on Single-Component AB and SOA Particles as well as Two-Component AB−SOA (by Mass Fraction) Particles[a]

aerosol	RH (%)	$10^4\gamma$
AB	50	146 ± 15
91:9 AB−SOA	47	26 ± 4
78:22 AB−SOA	48	18 ± 0.5
77:23 AB−SOA	45	20 ± 3
48:52 AB−SOA	46	6.2 ± 0.3
41:59 AB−SOA	47	6.6 ± 1.4
21:79 AB−SOA	46	3.0 ± 0.3
SOA	50	1.5 ± 0.2
SOA	30	1.7 ± 0.3
SOA	0	0.6 ± 0.2

[a] All experiments were conducted at approximately equivalent relative humidities, except for those with pure SOA at 0% and 30% RH.

single-point decays with the mixed composition particles, the uncertainties were calculated by propagating errors in the first-order rate constants through to the calculated slope of the k^I versus surface area plot. In addition, we believe the systematic and precision errors associated with the calculated inorganic mass fraction to be on the order of ±8% and ±12%, respectively. The former corresponds to errors pertaining to the value for the hygroscopic growth factor of the mixed aerosol, whereas the latter correlates to variability in the volume measurements of the ammonium bisulfate single-component and mixed aerosol experiments determined by the SMPS. We estimate that our systematic uncertainties in the uptake coefficients are generally larger, being on the order of ±30%. This estimate arises primarily from uncertainties in the aerosol surface areas, as well as from errors in the flow velocities and Brown correction procedure.[46]

The effects of the organic fraction on γ are represented in Figure 6, which shows the suppression in γ as a function of

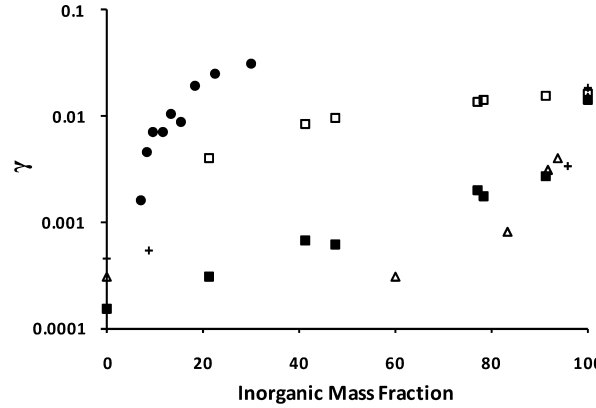

Figure 6. Uptake coefficients for N_2O_5 hydrolysis vs the inorganic mass fraction for this study at 50% RH (solid squares), ammonium sulfate and humic acid aerosols at 50% RH, Badger et al.[31] (open triangles), SOA-coated ammonium bisulfate aerosols at 60% RH, Folkers et al.[8] (plus signs), ambient aerosols measured in Seattle, WA, at 70% RH, Bertram et al.[27] (solid circles), and the results of the parametrization (open squares) developed by Bertram and Thornton[20] as applied to our data.

increasing particulate organic mass fraction. The results of Badger et al.[31] for humic acid and ammonium sulfate aerosol, Folkers et al.[8] for SOA and ammonium bisulfate aerosol, and Bertram et al.[27] for their field study investigating the organic to sulfate ratio in ambient aerosol in Seattle, WA, are also included in Figure 6 for easy comparison. Note that we obtained the values from Folkers et al.[8] through the same approach outlined above, assuming inorganic fractions of 5% and 7% by volume, as stated by the authors.[8] We received the data of Bertram et al.[27] directly from the researchers. In addition, we have also included the results of the parametrization developed by Bertram and Thornton[20] as applied to our data.

4. Discussion

The ability of an organic component to suppress N_2O_5 hydrolysis when added to a soluble inorganic has been previously addressed by other researchers.[8,13,16−19,21] Our results indicate that N_2O_5 uptake is slower on aerosol containing an organic fraction, with a large suppression in γ occurring even for aerosol with a small SOA fraction. It is evident from Figures 4 and 5 that only a small quantity of ammonium bisulfate aerosol is required to induce a large decay and thus lead to a large uptake coefficient. Conversely, large aerosol surface areas were necessary to measure the small γ in the SOA single-component experiments.

These results indicate that aqueous ammonium bisulfate is highly reactive, producing a $\gamma = 1.5 \times 10^{-2} \pm 1.5 \times 10^{-3}$, 1−2 orders of magnitude larger than all other γ values obtained for this study. This uptake coefficient is in agreement with other aqueous systems, both AB and non-AB systems. In fact, researchers[8,48−50] who have investigated ammonium bisulfate particles at relative humidity conditions of 48−60% have reported a very narrow range of $\gamma = 0.016-0.018$, whereas only two investigations have reported higher values: those of Bertram and Thornton[20] ($\gamma = 0.028$, 60% RH) and Mozurkewich and Calvert[6] ($\gamma = 0.05$, 50% RH). We consider these values as upper thresholds to the uptake coefficient of N_2O_5 on aqueous AB particles. The Bertram and Thornton result may be higher due to a low nitrate effect, arising from the very low N_2O_5 mixing ratios used.[20] If we compare our result against those for non-AB aqueous systems under similar wet conditions, we find that N_2O_5 hydrolysis conducted on ammonium sulfate,[7,8,31,48,49]

sodium nitrate,[9,49] NaCl/artificial seawater,[13−15] and malonic acid[11] aerosols produces γ values of 0.010−0.044, 0.00042−0.0032, 0.0102−0.035, and 0.018, respectively. Thus, with the exception of the sodium nitrate experiments, all γ values of both the AB and non-AB aqueous systems lie within the same order of magnitude and are relatively similar. The sodium nitrate results are at the lower end of the spectrum, as the uptake coefficients have been suppressed by large nitrate concentrations present in the aerosols.[9,49] We believe these comparisons generally validate our experimental technique.

The uptake coefficients we report for the SOA single-component experiments at 0%, 30%, and 50% RH are $6.0 \times 10^{-5} \pm 2.0 \times 10^{-5}$, $1.7 \times 10^{-4} \pm 3.0 \times 10^{-5}$, and $1.5 \times 10^{-4} \pm 2.0 \times 10^{-5}$, respectively. These very low values are not dissimilar to those reported by other researchers who have studied the hydrolysis reaction on pure complex organic substrates. In particular, we note that Folkers et al.[8] obtained a value of 4.5×10^{-4} (+0.015/−0.009) for SOA produced through the reaction of O_3 and α-pinene at 58% RH. To our knowledge, this is the only other uptake coefficient reported in the literature for SOA formed from the ozonolysis of α-pinene. The factor of 3 disagreement between the value reported here for SOA at 50% RH and that of Folkers et al. is possibly due to some systematic difference in experimental techniques between flow tube and chamber experiments, such as different compositions of SOA given that we form ours on a very short time scale at high precursor concentrations. However, we have recently compared the aerosol mass spectrometer (AMS) spectrum of the SOA formed in this manner[34] and found that it is similar to that of particles generated in chamber studies;[51] the O:C ratios of the SOA inferred from these investigations were similar: 0.26−0.34 for the flow tube approach[34] and about 0.25 for the chamber study.[51] Indeed these values indicate that the SOA examined in this study, similar to that of George et al.,[34] was fresh SOA that did not undergo oxidation and that it was similar in composition to both studies.[34,51] Thus, at this time we cannot fully explain the difference between the reported uptake coefficients for our SOA single-component study at 50% RH and the Folkers et al.[8] result.

We also observe a similarity between our values at 30% and 50% RH and the ones reported by Badger et al.[31] for reaction on a commercial (Aldrich) humic acid aerosol at 25% and 50% RH, $\gamma = 1 \times 10^{-4} \pm 1 \times 10^{-4}$ and $3 \times 10^{-4} \pm 1 \times 10^{-4}$, respectively. While certainly not the same complex mixture as that comprising α-pinene/O_3 SOA, it is noteworthy that the kinetics with humic acid particles are so comparable. Perhaps this arises because humic acid, as SOA, contains a wide range of oxygenated organic functional groups, such as carboxylic acids. In addition, the hygroscopic growth factors of SOA[35] and humic acid[43] at 50% RH are similarly small: 1.0 and 1.07, respectively.

In general, we note that very low γ values arise for these organic systems that exhibit low water content. Particularly, the reported uptake coefficient on solid malonic acid[11] particles is less than 0.001 for an RH of 10−50%. However, when an organic system takes up water, as in the case of aqueous malonic acid, the uptake coefficient is similar to that reported on aqueous inorganic systems and increases to $\gamma = 0.025$ at 50% RH.[11]

The results for the mixed AB−SOA aerosol obtained in this work are qualitatively in agreement with those of the two other studies of comparable systems (Figure 6). Specifically, the uptake coefficient for AB−SOA particles that were studied in the Folkers et al.[8] study was higher on the more inorganic-rich system: 3.4×10^{-3} (+0.15/−0.12) for 96:4 AB−SOA by mass fraction and 5.4×10^{-4} (+0.017/−0.012) for 9:91 AB−SOA. Interestingly, the comparison to the mixed ammonium sulfate−humic acid particle studies by Badger et al.[31] shows qualitatively the same behavior. In particular, we note that the uptake coefficients for ammonium bisulfate (this study) and ammonium sulfate[31] aerosols decreased by a factor of 5.6 and 4 upon the addition of less than 7% by mass fraction SOA and humic acid, respectively. In both cases, the decreases observed in γ thereafter occur in smaller degrees than the original decline and last level off at values almost identical to those of their single-component organic counterparts. It is interesting that similar kinetics arise from systems where the organics are either coated onto an inorganic substrate, as in our study, or initially mixed with the inorganics, as with Badger et al.[31]

We now consider two separate models to describe the suppression in the kinetics when organics are present. First, the initial large decline of the uptake coefficient may be due to a mass accommodation effect whereby the N_2O_5 is not as effectively taken up by the aerosol surface as it is on a purely inorganic aqueous surface. The surfactant-like properties of the individual components of the SOA and humic acid mixtures will give rise to this behavior. In this regard, we are in agreement with the conclusions of Badger et al.[31] Other researchers[13,16−19,21] have also attributed the decreases in N_2O_5 uptake to this effect, particularly those who have examined this process through organic monolayers. We also note that the subsequent, more gradual decline in reactivity with increasing organic fraction is possibly due to progressively lower water content on the surface. A second, alternate model of reactivity, recently presented, for example, by Anttila et al., is that the organic component in the particle is present as a phase-separated liquidlike layer on an inorganic aqueous spherical core.[52] As such, the particle consists of two phases, each of which has an associated partitioning (solubility) coefficient and diffusion coefficient. A mass accommodation coefficient is also associated with the organic coating. From this perspective, N_2O_5 hydrolysis occurs by mass accommodation into the particle surface, dissolution onto the organic coating, and then diffusion to the aqueous core. Anttila et al. tested their parametrization with aerosol chamber experiments using aqueous sulfate particles coated with monoterpene reaction products.[52] The researchers discovered that their model held most true to their empirical results for the cases in which the diffusion coefficient and solubility coefficient for the organic phase were at least 1 order of magnitude smaller than those of the aqueous phase. According to this model, the mass accommodation coefficient of the organic coating is not sufficiently reduced by the coat to account for the suppression in γ.[52] Rather, the decreases in the uptake coefficient are due to the small diffusion and solubility coefficients of the organic coating. Given the similarity of the Folkers et al.[8] results and those presented by Anttila et al.[52] to our own, this model and aerosol particle reactivity may well be an accurate description of the behavior seen in our experiments. At this point, we cannot unequivocally state whether the organic coating has its greatest effect in reducing γ by decreasing the mass accommodation coefficient of N_2O_5 into the organic phase or by hindering the dissolution and diffusion of N_2O_5 into the organic layer and aqueous layer, respectively, as a result of the inherently small solubility and diffusion coefficients of the organic coating.

We note that Bertram and Thornton have demonstrated that the water concentration in particles is a driving factor in the reactivity of mixed component aqueous systems.[20] To test this hypothesis, we applied the parametrization of Bertram and Thornton[20] to our mixed AB−SOA particle compositions to

model the behavior of γ as a function of nitrate and water concentrations. In particular, we assumed a nitrate concentration of 2 M, on the basis of the previous work of Thornton et al.[11] As these researchers calculated an upper limit for $[HNO_3]$ of 0.35 M for 30 ppb N_2O_5,[11] and since the average N_2O_5 concentration for our mixed aerosol experiments was ~180 ppb, we estimated an average nitrate concentration which scaled equivalently by a factor of 6. A nitrate concentration of 2 M is also the concentration that leads to a parametrized γ value equivalent to that of the empirical result for ammonium bisulfate at 50% RH. As with Bertram and Thornton, we calculated $[H_2O_{(l)}]$ using the aerosol inorganics model (AIM II), where we assume that the organics do not contribute significant water to the particles.[38,53]

The resulting uptake coefficients of the parametrization increased from 0.004 to 0.016 while the $[H_2O_{(l)}]$ increased from 7.2 to 27.1 M as the inorganic fraction increased. The results shown in Figure 6 (open squares) illustrate no sharp initial decline as with the empirical data, with relatively minor subsequent decreases compared to the laboratory results. This supports the contention that the kinetics suppression is due to a mechanism different from the processes parametrized by this model, probably driven by the different species present or by different particle morphologies.

Likewise, we note that direct measurements of the reactivity of N_2O_5 on ambient aerosol do not fully match the observations made in the laboratory. In particular, the results of Bertram and co-workers[27] illustrate that the uptake coefficient does indeed show a dependence on the organic mass fraction (Figure 6) at 70% RH for measurements obtained in Seattle, WA. The decline in the observed uptake coefficient with increasing organic mass fraction is not nearly as strong as that observed in the laboratory. The uptake coefficient drops from 0.031 to 0.0016 for inorganic:organic mass ratios ranging from 30:70 to 7:93, and the γ values are consistently much higher than all other laboratory results of mixed particles.[8,27,31] This could arise for a number of reasons. For example, the particles in Seattle may be externally mixed, such that a fraction of inorganic-rich particles keep the reactivity high, even in the presence of a substantial number of low-reactivity organic-rich particles, or there may be soluble inorganics present on the surface of the field particles. Although the researchers[27] note that the inorganic fraction is not entirely composed of ammonium sulfate and therefore may contain other inorganic material, it is unlikely that higher N_2O_5 reactivity occurs as a result of these unknown inorganics, since ammonium sulfates react as rapidly as any other inorganic substrate. Finally, the organics present in the field may be different from those in the laboratory, perhaps having been oxidatively processed at the surface, which will have increased their ability to take up water.

5. Conclusion and Atmospheric Implications

We report laboratory measurements of the uptake coefficient of N_2O_5 hydrolysis on ammonium bisulfate and SOA single-component particles as well as ammonium bisulfate−SOA mixed particles. Our values for the AB and SOA single-component studies are in agreement with previous work for both aqueous AB[8,48−50] and aqueous non-AB[7−9,11,13−15,31,48,49] systems and other organic experiments,[8,31] respectively. We observe a strong suppression in γ upon the addition of increasingly larger organic fractions, with the most notable decrease occurring between pure AB particles and the addition of a small organic fraction. This initial decline suggests that mass accommodation is possibly inhibited with the inclusion of organics in the particle. Alternatively, Anttila et al.[52] present a model suggesting that organic coatings form on inorganic particle cores, a model which may also describe our results.

From an atmospheric modeling perspective, the models demonstrate that their results are sensitive to the N_2O_5 uptake coefficient down to values of at least 10^{-3} and perhaps even lower,[1−5] so deciphering the role of organics in suppressing the room temperature uptake coefficient from values above 10^{-2}, as present with soluble inorganic and small organics, is very important. It does appear, however, that the reactivity on a purely biogenic organic particle, which demonstrates uptake coefficients of 10^{-4}, is unlikely to significantly impact atmosphere processes or influence model calculations to a high degree. Given that ambient measurements do not directly match the behavior demonstrated in the few laboratory studies of mixed composition particles, the mechanism by which organics suppress N_2O_5 heterogeneous reactivity within the atmosphere needs to be better determined before it can be included in atmospheric models.

Acknowledgment. This project was financially supported by the NSERC. The building of the new CIMS instrument was supported by the NSERC and the Ontario Ministry of the Environment. Such support does not indicate endorsement by the Ministry of the contents of this material. We acknowledge the support of G. Huey and D. Tanner (Georgia Institute of Technology) for their designs for the CIMS, as well as Glenn Wolfe (University of Washington) for the data acquisition program for the CIMS and Joel Thornton for discussions.

References and Notes

(1) Evans, M. J.; Jacob, D. J. *Geophys. Res. Lett.* [Online] **2005**, *32*, DOI 10.1029/2005GL022469. http://www.agu.org.myaccess.library.utoronto.ca/journals/gl/gl0509/2005GL022469/2005GL022469.pdf, accessed July 25, 2010.

(2) Dentener, F. J.; Crutzen, P. J. *J. Geophys. Res.* **1993**, *98*, 7149–7163.

(3) Davis, J. M.; Bhave, P. V.; Foley, K. M. *Atmos. Chem. Phys.* **2008**, *8*, 5295–5311.

(4) Riemer, N.; Vogel, H.; Vogel, B.; Anttila, T.; Kiendler-Scharr, A.; Mentel, T. F. *J. Geophys. Res.* [Online] **2009**, *114*, DOI 10.1029/2008JD011369. http://www.agu.org.myaccess.library.utoronto.ca/journals/jd/jd0917/2008JD011369/2008JD011369.pdf, accessed July 25, 2010.

(5) Liao, H.; Seinfeld, J. H. *J. Geophys. Res.* [Online] **2005**, *110*, DOI 10.1029/2005JD005907. http://www.agu.org.myaccess.library.utoronto.ca/journals/jd/jd0518/2005JD005907/2005JD005907.pdf, accessed October 13, 2010.

(6) Mozurkewich, M.; Calvert, J. G. *J. Geophys. Res.* **1988**, *93*, 15889–15896.

(7) Hu, J. H.; Abbatt, J. P. D. *J. Phys. Chem. A* **1997**, *101*, 871–878.

(8) Folkers, M.; Mentel, T. F.; Wahner, A. *Geophys. Res. Lett.* [Online] **2003**, *30*, DOI 10.1029/2003GL017168. http://www.agu.org.myaccess.library.utoronto.ca/journals/gl/gl0312/2003GL017168/2003GL017168.pdf, accessed March 3, 2010.

(9) Mentel, T. F.; Sohn, M.; Wahner, A. *Phys. Chem. Chem. Phys.* **1999**, *1*, 5451–5457.

(10) Wahner, A.; Mentel, T. F.; Sohn, M.; Stier, J. *J. Geophys. Res.* **1998**, *103*, 31103–31112.

(11) Thornton, J. A.; Braban, C. F.; Abbatt, J. P. D. *Phys. Chem. Chem. Phys.* **2003**, *5*, 4593–4603.

(12) Griffiths, P. T.; Badger, C. L.; Cox, R. A.; Folkers, M.; Henk, H. H.; Mentel, T. F. *J. Phys. Chem. A* **2009**, *113*, 5082–5090.

(13) Thornton, J. A.; Abbatt, J. P. D. *J. Phys. Chem. A* **2005**, *109*, 10004–10012.

(14) Behnke, W.; George, C.; Scheer, V.; Zetzsch, C. *J. Geophys. Res.* **1997**, *102*, 3795–3804.

(15) Stewart, D. J.; Griffiths, P. T.; Cox, R. A. *Atmos. Chem. Phys.* **2004**, *4*, 1381–1388.

(16) McNeill, V. F.; Wolfe, G. M.; Thornton, J. A. *J. Phys. Chem. A* **2007**, *111*, 1073–1083.

(17) McNeill, V. F.; Patterson, J.; Wolfe, G. M.; Thornton, J. A. *Atmos. Chem. Phys.* **2006**, *6*, 1635–1644.

(18) Park, S. C.; Burden, D. K.; Nathanson, G. M. *J. Phys. Chem. A* **2007**, *111*, 2921–2929.

(19) Cosman, L. M.; Bertram, A. K. *J. Phys. Chem. A* **2008**, *112*, 4625–4635.
(20) Bertram, T. H.; Thornton, J. A. *Atmos. Chem. Phys.* **2009**, *9*, 8351–8363.
(21) Cosman, L. M.; Knopf, D. A.; Bertram, A. K. *J. Phys. Chem. A* **2008**, *112*, 2386–2396.
(22) Lawrence, J. R.; Glass, S. V.; Park, S. C.; Nathanson, G. M. *J. Phys. Chem. A* **2005**, *109*, 7458–7465.
(23) Däumer, B.; Niessner, R.; Klockow, D. *J. Aerosol Sci.* **1992**, *23*, 315–325.
(24) Lawrence, J. R.; Glass, S. V.; Nathanson, G. M. *J. Phys. Chem. A* **2005**, *109*, 7449–7457.
(25) Stemmler, K.; Vlasenko, A.; Guimbaud, C.; Ammann, M. *Atmos. Chem. Phys.* **2008**, *8*, 5127–5141.
(26) Gilman, J. B.; Vaida, V. *J. Phys. Chem. A* **2006**, *110*, 7581–7587.
(27) Bertram, T. H.; Thornton, J. A.; Riedel, T. P.; Middlebrook, A. M.; Bahreini, R.; Bates, T. S.; Quinn, P. K.; Coffman, D. J. *Geophys. Res. Lett.* [Online] **2009**, *36*, DOI 10.1029/2009GL040248. http://www.agu.org.myaccess.library.utoronto.ca/journals/gl/gl0919/2009GL040248/2009GL040248.pdf, accessed March 3, 2010.
(28) Brown, S. S.; Ryerson, T. B.; Wollny, A. G.; Brock, C. A.; Peltier, R.; Sullivan, A. P.; Weber, R. J.; Dubé, W. P.; Trainer, M.; Meagher, J. F.; Fehsenfeld, F. C.; Ravishankara, A. R. *Science* **2006**, *311*, 67–70.
(29) Brown, S. S.; Stark, H.; Ciciora, S. J.; McLaughlin, R. J.; Ravishankara, A. R. *Rev. Sci. Instrum.* **2002**, *73*, 3291–3301.
(30) Brown, S. S.; Dibb, J. E.; Stark, H.; Aldener, M.; Vozella, M.; Whitlow, S.; Williams, E. J.; Lerner, B. M.; Jakoubek, R.; Middlebrook, A. M.; DeGouw, J. A.; Warneke, C.; Goldan, P. D.; Kuster, W. C.; Angevine, W. M.; Sueper, D. T.; Quinn, P. K.; Bates, T. S.; Meagher, J. F.; Fehsenfeld, F. C.; Ravishankara, A. R. *Geophys. Res. Lett.* [Online] **2004**, *31*, DOI 10.1029/2004GL019412. http://www.agu.org.myaccess.library.utoronto.ca/journals/gl/gl0407/2004GL019412/2004GL019412.pdf, accessed October 13, 2010.
(31) Badger, C. L.; Griffiths, P. T.; George, I.; Abbatt, J. P. D.; Cox, R. A. *J. Phys. Chem. A* **2006**, *110*, 6986–6994.
(32) Zhang, Q.; Jimenez, J. L.; Canagaratna, M. R.; Allan, J. D.; Coe, H.; Ulbrich, I.; Alfarra, M. R.; Takami, A.; Middlebrook, A. M.; Sun, Y. L.; Dzepina, K.; Dunlea, E.; Docherty, K.; DeCarlo, P. F.; Salcedo, D.; Onasch, T.; Jayne, J. T.; Miyoshi, T.; Shimono, A.; Hatakeyama, S.; Takegawa, N.; Kondo, Y.; Schneider, J.; Drewnick, F.; Borrmann, S.; Weimer, S.; Demerjian, K.; Williams, P.; Bower, K.; Bahreini, R.; Cottrell, L.; Griffin, R. J.; Rautiainen, J.; Sun, J. Y.; Zhang, Y. M.; Worsnop, D. R. *Geophys. Res. Lett.* [Online] **2007**, *34*, DOI 10.1029/2007GL029979. http://www.agu.org.myaccess.library.utoronto.ca/journals/gl/gl0713/2007GL029979/2007GL029979.pdf, accessed April 21, 2010.
(33) Kercher, J. P.; Riedel, T. P.; Thornton, J. A. *Atmos. Meas. Tech.* **2009**, *2*, 193–204.
(34) George, I. J.; Abbatt, J. P. D. *Atmos. Chem. Phys.* **2010**, *10*, 5551–5563.
(35) Wex, H.; Petters, M. D.; Carrico, C. M.; Hallbauer, E.; Massling, A.; McMeeking, G. R.; Poulain, L.; Wu, Z.; Kreidenweis, S. M.; Stratmann, F. *Atmos. Chem. Phys.* **2009**, *9*, 3987–3997.
(36) Seinfeld, J. H.; Pandis, S. N. *Atmospheric Chemistry and Physics: From Air Pollution to Climate Change*; John Wiley & Sons, Inc.: New York, 1998.
(37) Tang, I. N.; Munkelwitz, H. R. *J. Geophys. Res.* **1994**, *99*, 18801–18808.
(38) Clegg, S. L.; Brimblecombe, P. *J. Phys. Chem. A* **1998**, *102*, 2137–2154.
(39) *CRC Handbook of Chemistry and Physics*, 90th ed.; Lide, D. R., Ed.; CRC Press/Taylor and Francis: Boca Raton, FL, 2010.
(40) Kostenidou, E.; Pathak, R. K.; Pandis, S. N. *Aerosol Sci. Technol.* **2007**, *41*, 1002–1010.
(41) Stokes, R. H.; Robinson, R. A. *J. Phys. Chem.* **1966**, *70*, 2126–2130.
(42) Zdanovskii, A. *Zh. Fiz. Khim.* **1948**, *22*, 1475–1485.
(43) Badger, C. L.; George, I.; Griffiths, P. T.; Braban, C. F.; Cox, R. A.; Abbatt, J. P. D. *Atmos. Chem. Phys.* **2006**, *6*, 755–768.
(44) Brooks, S. D.; DeMott, P. J.; Kreidenweis, S. M. *Atmos. Environ.* **2004**, *38*, 1859–1868.
(45) Gysel, M.; Crosier, J.; Topping, D. O.; Whitehead, J. D.; Bower, K. N.; Cubison, M. J.; Williams, P. I.; Flynn, M. J.; McFiggans, G. B.; Coe, H. *Atmos. Chem. Phys.* **2007**, *7*, 6131–6144.
(46) Brown, R. L. *J. Res. Natl. Bur. Stand.* **1978**, *83*, 1–8.
(47) Fuchs, N. A.; Sutugin, A. G. *Highly Dispersed Aerosols*; Ann Arbor Science Publishers: Ann Arbor, MI, 1970.
(48) Kane, S. M.; Caloz, F.; Leu, M. T. *J. Phys. Chem. A* **2001**, *105*, 6465–6470.
(49) Hallquist, M.; Stewart, D. J.; Stephenson, S. K.; Cox, R. A. *Phys. Chem. Chem. Phys.* **2003**, *5*, 3453–3463.
(50) Griffiths, P. T.; Cox, R. A. *Atmos. Sci. Lett.* **2009**, *10*, 159–163.
(51) Bahreini, R.; Keywood, M. D.; Ng, N. L.; Varutbangkul, V.; Gao, S.; Flagan, R. C.; Seinfeld, J. H.; Worsnop, D. R.; Jimenez, J. L. *Environ. Sci. Technol.* **2005**, *39*, 5674–5688.
(52) Anttila, T.; Kiendler-Scharr, A.; Tillmann, R.; Mentel, T. F. *J. Phys Chem. A* **2006**, *110*, 10435–10443.
(53) Carslaw, K. S.; Clegg, S. L.; Brimblecombe, P. *J. Phys. Chem.* **1995**, *99*, 11557–11574.

JP107721V